Inexact Convex Relaxations for AC Optimal Power Flow: Towards AC Feasibility

Andreas Venzke, *Student Member, IEEE,* Spyros Chatzivasileiadis, *Senior Member, IEEE,* and Daniel K. Molzahn, *Member, IEEE*

***Abstract*—Convex relaxations of AC optimal power flow (AC-OPF) problems have attracted significant interest as in several instances they provably yield the global optima to the original non-convex problems. If the relaxation fails to be exact, the optimality gap is often small, i.e., the relaxation's objective function value is close to the objective value of the best known AC-feasible point. This work studies inexact solutions to the quadratic convex (QC) and semidefinite (SDP) relaxations, providing a comprehensive analysis on the resulting distances to both AC-feasibility and local optimality. To this end, we propose two empirical distance metrics which complement the optimality gap. In addition, we investigate two methods to recover AC-feasible solutions: penalization methods and warm-starting of non-convex solvers. For the PGLib OPF benchmarks, we show that i) despite an optimality gap of less than 1%, several test cases still exhibit substantial distances to AC-feasibility and local optimality; ii) the optimality gaps do not strongly correlate with either distance. We also show that several existing penalization methods may fail to recover AC-feasible or near-globally optimal solutions and that benefits of warm-starting of local solvers strongly depend on test case and solver and are not correlated with the optimality gaps.**

***Index Terms*—Convex quadratic optimization, optimal power flow, nonlinear programming, semidefinite programming.**

I. Introduction

The AC optimal power flow (AC-OPF) problem is a key tool for the efficient operation of power systems [1]. The AC-OPF problem minimizes an objective function (e.g., generation cost) subject to the power system operational constraints (e.g., limits on the transmission line flows and bus voltages). Nonlinearities from the AC power flow equations result in the AC-OPF problem being non-convex and generally NP-hard, even for tree network topologies [2]. If solved with a non-convex solver, first, there is no guarantee that the solver identifies a feasible solution even if it exists and, second, there is no guarantee an obtained solution corresponds to the global optimum. Since solver reliability is very important, most system operators currently use the DC power flow approximation, which neglects voltage magnitudes, reactive power, and active power losses in order to obtain a linear or quadratic program. The DC-OPF approximation can exhibit substantial errors [3], particularly for stressed system conditions.

A. Venzke and S. Chatzivasileiadis are with the Department of Electrical Engineering, Technical University of Denmark, 2800 Kgs. Lyngby, Denmark e-mail: {andven, spchatz}@elektro.dtu.dk.

D. K. Molzahn is with the School of Electrical and Computer Engineering, Georgia Institute of Technology, Atlanta, GA 30313, USA as well as the Energy Systems Division, Argonne National Laboratory, Lemont, IL 60439 USA, e-mail: molzahn@gatech.edu.

This work is supported by the multiDC project, funded by Innovation Fund Denmark, Grant Agreement No. 6154-00020B as well as by the U.S. Department of Energy, Office of Electricity Delivery and Energy Reliability under contract DE-AC-02-06CH11357.

In the last decade, different convex relaxations of the AC-OPF problem have been proposed, including second-order cone programming (SOCP) [4], semidefinite programming (SDP) [5], [6], and quadratic convex (QC) relaxations [7]. A recent survey is available in [8]. These relaxations have attained significant interest as in several test cases they provably yield the global optimum to the original non-convex problem [6], [9], i.e., they are exact, and are shown to be tractable for test cases with thousands of buses [7], [9], [10]. Besides obtaining a global optimality certificate, solving a convex instead of a non-convex problem has major advantages in various applications of AC-OPF problems. For example, several decomposition techniques are only guaranteed to converge for convex problems [11], and bi-level programs arising in AC-OPF under uncertainty are more tractable [12], [13].

If, however, the convex relaxations of AC-OPF problems are inexact, only conservative lower bounds on the objective values are obtained, and the solutions are not AC-feasible. Previous works (e.g., [7]) have shown that the obtained lower bounds on the objective values are often quite close to the solutions of non-convex solvers, i.e., the optimality gaps are less than 1% for many problems. To obtain an AC-feasible or an optimal solution from an inexact convex relaxation, different methods have been proposed in the literature, including moment hierarchies [14] and objective function penalizations [15]–[17]. Higher-order moment relaxations generalize the SDP relaxation of [6], facilitating global solutions to a broader class of problems at the computational cost of larger SDP constraints [14]. Augmenting the objective function with penalty terms based on, e.g., reactive power [15] can result in near-globally optimal solutions for various test cases.

Most of the previous works (e.g., [7], [16]) related to convex relaxations of AC-OPF problems have focused on the optimality gap as the main measure for the tightness of the relaxation. However, if the relaxation is inexact, the magnitude of the optimality gap does not directly provide a measure for the distance to feasibility or local optimality to the original non-convex AC-OPF problem. To this end, the purpose of this work is to provide a comprehensive study on the resulting distance of the inexact solutions of the QC and SDP relaxations. In addition, we investigate two methods for recovering AC-feasible and locally optimal solutions from inexact solutions: penalization methods and warm-starting of non-convex solvers. For our comprehensive study, we use a wide range of test cases from the PGLib OPF benchmarks v18.08 [18]. The main contributions of our work are:

1) This is the first work to provide an in-depth analysis on the distance of the decision variables for the QC

and SDP relaxations to both AC-feasibility and local optimality for the original non-convex AC-OPF problem. We propose two empirical metrics as alternatives to the optimality gap for analyzing the tightness of the relaxations: i) the cumulative normalized constraint violation, and ii) the average normalized distance to local optimality. We show that these metrics are not strongly correlated with the optimality gap and that despite having an optimality gap of less than 1%, several test instances still exhibit substantial distances to AC-feasibility and local optimality.

2) We provide a rigorous analysis of three different penalization methods for the SDP relaxation for a wide range of PGLib OPF test cases. We find that the penalization methods are able to recover AC-feasible solutions but the incurred sub-optimality by modifying the original objective function can be significant. In addition, none of the penalization methods are successful at obtaining AC-feasible solutions for several test cases.
3) To improve robustness and speed of solving AC-OPF, we investigate warm-starting of non-convex solvers with the solutions to the inexact convex relaxations. We show that the benefits in terms of computational speed, solver reliability, and solution quality strongly depend on the solver and test case. For the considered PGLib OPF test cases, the warm-started interior point solver in IPOPT [19] achieves the best performance out of the investigated methods. It exhibits a computational speed-up in the majority of test cases while the solver reliability and solution quality are preserved.

This paper is structured as follows: In Section II, we state the formulations of the AC-OPF problem and the considered QC and SDP relaxations. Section II proposes two metrics to assess the distance to AC-feasibility and local optimality of inexact convex relaxations. Section III presents different methods for recovering AC-feasible or locally optimal solutions from inexact convex relaxations. Section V provides extensive computational studies using the PGLib OPF benchmarks. Section VI concludes and provides directions for further research.

II. AC Optimal Power Flow and Relaxations

The AC-OPF problem has a variety of different mathematically equivalent formulations. For a detailed survey on AC-OPF and convex relaxations, the reader is referred to [8]. Here, for brevity, we follow the AC-OPF formulation of [7] to facilitate the derivation of the SDP and QC relaxations.

A power grid consists of the set $\mathcal{N}$ of buses, a subset of those denoted by $\mathcal{G}$ have a generator. The buses are connected by a set $(i,j) \in \mathcal{L}$ of power lines from bus i to j. The optimization variables are the complex bus voltages V_k for each bus $k \in \mathcal{N}$ and the complex power dispatch of generator S_{G_k} for each bus $k \in \mathcal{G}$. The objective function f_{cost} minimizes the cost associated with active power dispatch:

$$\min_{V,S_G} \; f_{\text{cost}} := \sum_{k\in\mathcal{G}} c_{k_2} \Re\{S_{G_k}\}^2 + c_{k_1} \Re\{S_{G_k}\} + c_{k_0} \qquad (1)$$

The terms c_{k_2}, c_{k_1} and c_{k_0} denote quadratic, linear and constant cost terms associated with generator active power dispatch, respectively. The following constraints are enforced:

$$(V_k^{\min})^2 \le V_k V_k^* \le (V_k^{\max})^2 \qquad \forall k \in \mathcal{N} \qquad (2a)$$
$$S_{G_k}^{\min} \le S_{G_k} \le S_{G_k}^{\max} \qquad \forall k \in \mathcal{G} \qquad (2b)$$
$$|S_{ij}| \le S_{ij}^{\max} \qquad \forall (i,j) \in \mathcal{L} \qquad (2c)$$
$$S_{G_k} - S_{D_k} = \sum_{(k,j)\in\mathcal{L}} S_{kj} \qquad \forall k \in \mathcal{N} \qquad (2d)$$
$$S_{ij} = Y_{ij}^* V_i V_i^* - Y_{ij}^* V_i V_j^* \qquad \forall (i,j) \in \mathcal{L} \qquad (2e)$$
$$-\theta_{ij}^{\max} \le \angle(V_i V_j^*) \le \theta_{ij}^{\max} \qquad \forall (i,j) \in \mathcal{L} \qquad (2f)$$

The bus voltage magnitudes are constrained in (2a) by upper and lower limits $V_k^{\min}$ and $V_k^{\max}$. The superscript $*$ denotes the complex conjugate. Similarly, the generators' complex power outputs are limited in (2b) by upper and lower bounds $S_{G_k}^{\min}$ and $S_{G_k}^{\max}$, where inequality constraints for complex variables are interpreted as bounds on the real and imaginary parts. The apparent branch flow S_{ij} is upper bounded in (2c) by $S_{ij}^{\max}$. The nodal complex power balance (2d) including the load S_D has to hold for each bus. The apparent branch flow S_{ij} is defined in (2e). The term Y denotes the admittance matrix of the power grid. The branch flow is also limited in (2f) by an upper limit on the angle difference $\theta_{ij}^{\max}$. As proposed in [6], [7], an additional auxiliary matrix variable W is introduced, which denotes the product of the complex bus voltages:

$$W_{ij} = V_i V_j^* \qquad (3)$$

This facilitates the reformulation of (2a), (2e), and (2f) as:

$$(V_k^{\min})^2 \le W_{kk} \le (V_k^{\max})^2 \qquad \forall k \in \mathcal{N} \qquad (4a)$$
$$S_{ij} = Y_{ij}^* W_{ii} - Y_{ij}^* W_{ij} \qquad \forall (i,j) \in \mathcal{L} \qquad (4b)$$
$$S_{ij} = Y_{ij}^* W_{jj} - Y_{ij}^* W_{ij}^* \qquad \forall (i,j) \in \mathcal{L} \qquad (4c)$$
$$\tan(-\theta_{ij}^{\max}) \le \tfrac{\Re\{W_{ij}\}}{\Im\{W_{ij}\}} \le \tan(\theta_{ij}^{\max}) \qquad \forall (i,j) \in \mathcal{L} \qquad (4d)$$

The only source of non-convexity is the voltage product (3).

A. DC Optimal Power Flow (DC-OPF) Approximation

The DC-OPF, which serves here as benchmark, is an approximation that is often used in, e.g., electricity markets and unit commitment problems. This approximation neglects voltage magnitudes, reactive power, and active power losses. The state variables are the active generation P_G and the voltage angles θ. Depending on whether a quadratic cost term is included, the optimization problem is either a linear program (LP) or a quadratic program (QP). For brevity the formulation is omitted, but can be found in, e.g., [3]. The DC-OPF problem approximates but is not a relaxation of the AC-OPF problem.

B. Quadratic Convex (QC) Relaxation

The QC relaxation proposed in [7] uses convex envelopes of the polar representation of the AC-OPF problem to relax the dependencies among voltage variables. The non-convex constraint (3) is removed; variables for voltages, $v_i \angle\theta_i \; \forall i \in \mathcal{N}$, and squared current flows, $l_{ij} \; \forall (i,j) \in \mathcal{L}$, are added; and convex constraints and envelopes are introduced [7]:

$$W_{kk} = \left\langle v_k^2 \right\rangle^T \qquad \forall k \in \mathcal{N} \qquad (5a)$$
$$\Re\{W_{ij}\} = \left\langle \langle v_i v_j \rangle^M \left\langle \cos(\theta_i - \theta_j) \right\rangle^C \right\rangle^M \qquad \forall (i,j) \in \mathcal{L} \qquad (5b)$$

$$\Im\{W_{ij}\} = \left\langle \langle v_i v_j \rangle^M \langle \sin(\theta_i - \theta_j) \rangle^S \right\rangle^M \quad \forall (i,j) \in \mathcal{L} \quad (5c)$$

$$S_{ij} + S_{ji} = Z_{ij} l_{ij} \quad \forall (i,j) \in \mathcal{L} \quad (5d)$$

$$|S_{ij}|^2 \leq W_{ii} l_{ij} \quad \forall (i,j) \in \mathcal{L} \quad (5e)$$

The superscripts T, M, C, S denote convex envelopes for the square, bilinear product, cosine, and sine functions, respectively; for details, see [7]. The term Z_{ij} denotes the line impedance. The resulting optimization problem is an SOCP that minimizes (1) subject to (2b) – (2d), (4), and (5). The QC relaxation dominates the SOCP relaxation of [4] in terms of tightness at a similar computational complexity, and is particularly effective for meshed transmission networks with tight angle constraints. We therefore omit the SOC relaxation.

C. Semidefinite (SDP) Relaxation

In the semidefinite (SDP) relaxation proposed in [5], [6], the non-convex constraint (3) is reformulated in matrix form:

$$W \succeq 0 \quad (6a)$$

$$\text{rank}(W) = 1 \quad (6b)$$

The non-convexity of the resulting formulation is encapsulated in the rank constraint (6b), which is subsequently relaxed. The resulting optimization is an SDP that minimizes the objective function (1) subject to (2b) – (2d), (4), and (6a). In terms of theoretical tightness, the QC neither dominates nor is dominated by the SDP relaxation [7].

III. Distance Metrics for Inexact Solutions

The optimality gap is a widely used distance metric for assessing the quality of inexact solutions obtained from convex relaxations. The optimality gap between the solution to the convex relaxation and the best known feasible point for the non-convex AC-OPF problem is defined as follows:

$$(1 - \tfrac{f_{\text{cost}}^{\text{relax}}}{f_{\text{cost}}^{\text{local}}}) \times 100\% \quad (7)$$

The term $f_{\text{cost}}^{\text{relax}}$ denotes the lower objective value bound from the relaxation and $f_{\text{cost}}^{\text{local}}$ is the objective value of the best known feasible point obtained from a local non-convex solver. If the relaxation is inexact, the magnitude of the optimality gap does not necessarily indicate the decision variables' distances to feasibility or local optimality for the original non-convex AC-OPF problem; e.g., for cases with very flat objective functions, solutions with small optimality gaps could still exhibit substantial distances to both. Additionally, the closest solution that is AC-feasible might not coincide with the closest locally optimal solution. To assess both these distances for a wide range of test cases, we propose two new alternative metrics: i) the cumulative normalized constraint violation and ii) the average normalized distance to a local solution.

A. Cumulative Normalized Constraint Violation

To assess the distance to AC-feasibility, we run an AC power flow (AC-PF) with set-points obtained from an inexact convex relaxation and evaluate the constraint violations. For each bus $k \in \mathcal{N}$, there are four state variables: the voltage magnitude $|V_k|$, the voltage angle θ_k, the active power injection $\Re\{S_{Gk} - S_{Dk}\}$, and the reactive power injection $\Im\{S_{Gk} - S_{Dk}\}$. If the solution to the convex relaxation is inexact, the resulting state variables do not fulfill the AC power flow equations and are hence AC-infeasible. To recover a solution that satisfies the AC power flow equations, an AC power flow (AC-PF) can be computed with the set-points obtained from the convex relaxation. We choose to use the setpoints for active power injections and voltage magnitudes at generator buses given by the relaxation's solution.

We propose the cumulative normalized constraint violation resulting from this power flow solution as a metric to quantify the distance to AC-feasibility. This metric can be computed by taking the sum of constraint violations from the AC-PF solution, normalized by the respective upper and lower constraint bounds. Using as example the AC-PF bus voltages $|V_k^{\text{AC-PF}}|$, we define the cumulative normalized voltage violations V_{viol}:

$$V_{\text{viol}} := \sum_{k \in \mathcal{N}} \frac{\max(|V_k^{\text{AC-PF}}| - V_k^{\max}, V_k^{\min} - |V_k^{\text{AC-PF}}|, 0)}{V_k^{\max} - V_k^{\min}} \times 100\% \quad (8)$$

We found that this metric carries more information than assessing the average or maximum constraint violations since only a small subset of the constraints are active in typical AC-OPF problems. This metric allows for a comparison of the distance to AC-feasibility among relaxations for a given system. Note that it is not averaged by the number of buses, and as a result, inexact convex relaxations of the AC-OPF for larger systems may exhibit larger values.

B. Average Normalized Distance to a Local Solution

To assess the distance to local optimality, we propose an additional metric defined as the averaged normalized distance of the variable values obtained with the inexact convex relaxation to a locally optimal solution obtained with a non-convex solver. This metric can be computed by taking the absolute difference between the variable value from the relaxation's solution and the value from the local optimum, normalized by the difference in the upper and lower variable bound, and then averaging over all variables. As this metric is averaged by the number of variables, which is a function of the system size, it allows for fair comparison among relaxations for systems with different sizes. As an example, we define the average normalized distance V_{dist} of the bus voltage magnitudes in the relaxation $|V_k^{\text{relax}}|$ to the local optimum $|V_k^{\text{opt}}|$ as:

$$V_{\text{dist}} := \tfrac{1}{|\mathcal{N}|} \sum_{k \in \mathcal{N}} \frac{\left| |V_k^{\text{relax}}| - |V_k^{\text{opt}}| \right|}{V_k^{\max} - V_k^{\min}} \times 100\% \quad (9)$$

IV. Recovery of AC-Feasible and Locally Optimal Solutions

We present two methods to recover AC-feasible or locally optimal solutions from inexact convex relaxations: penalization methods and warm-starting of non-convex solvers.

A. Penalization Methods for SDP Relaxation

For a variety of test cases, the SDP relaxation has a small optimality gap but the obtained solution W does not fulfill the rank-1 condition (6b); see, e.g., [15]. To drive the solution

towards a rank-1 point in order to recover an AC-feasible solution, several works [15], [16] have proposed augmenting the objective function of the semidefinite relaxation with penalty terms, denoted with f_{pen}. Note that the penalized formulations *are not* relaxations of the original AC-OPF problem, but can still be useful for recovering feasible points. We focus on the following three penalty terms. First, the nuclear norm proposed by [20] is a widely used penalty term for the general rank-minimization problem:

$$f_{\text{pen}} = f_{\text{cost}} + \epsilon_{\text{pen}} \text{Tr}\{W\} \tag{10}$$

The penalty weight is denoted with ϵ_{pen} and the term $\text{Tr}\{\cdot\}$ indicates the trace of the matrix W, i.e., the sum of the diagonal elements. Second, specific for the AC-OPF, the work in [15] proposes penalization of the reactive generator outputs:

$$f_{\text{pen}} = f_{\text{cost}} + \epsilon_{\text{pen}} \sum_{k \in \mathcal{G}} \Im\{S_{G_k}\} \tag{11}$$

Finally, the work in [16] suggests adding an apparent branch flow loss penalty to the objective function:

$$f_{\text{pen}} = f_{\text{cost}} + \epsilon_{\text{pen}} \sum_{(i,j) \in \mathcal{L}} |S_{ij} - S_{ji}| \tag{12}$$

Both the works [15], [16] show that certain choices of ϵ_{pen} result in successful recovery of an AC-feasible and near-globally optimal operating points for selected test cases. In Section V-C, we will present a counterexample and provide a detailed empirical analysis of the different penalty terms for a wide range of test cases. Note that to the knowledge of the authors, penalization methods have not been applied to address inexact solutions resulting from the QC relaxation.

B. Warm-Starting Non-Convex Local Solvers

When penalization methods are not successful at recovering a rank-1 solution, non-convex solvers can be warm started with the solution of convex relaxations in order to recover an AC-feasible and locally optimal solution. Compared to a flat start of $V_k = 1\angle 0$, $\forall k \in \mathcal{N}$, which is a common initialization for non-convex solvers, warm-starting could lead to i) reduced computational time and ii) improved solution quality. For these purposes, we utilize two types of non-convex solvers:

1) Sequential Quadratic Programming (SQP): To compute a search direction, this method iteratively solves second-order Taylor approximations of the Lagrangian which are formulated as Quadratic Programs (QP). Line-search or other methods are used to determine an appropriate step size. In theory, this solution method is well suited for being warm-started [21]. We will use KNITRO [22] as the reference SQP solver.

2) Interior-Point Methods (IPM): To deal with the constraint inequalities in the optimization problem, a logarithmic barrier term is added to the objective function with a multiplicative factor. This factor is decreased as the interior-point method converges, and the resulting barrier term resembles the indicator function. Interior point methods are challenging to efficiently warm start since the logarithmic barrier term initially keeps the solution away from inequality constraints that are binding at optimality [23]. We will use both KNITRO [22] and IPOPT [19] as reference IPM solvers.

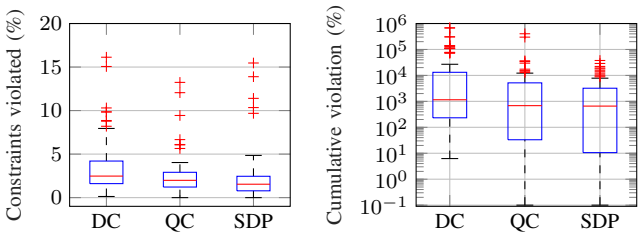

Fig. 1. The overall share of constraints violated and the cumulative normalized constraint violation in the AC-PF with the generators' setpoints for active power outputs and voltage magnitudes fixed to the values obtained from the DC-OPF, the QC relaxation, and the SDP relaxation.

V. Simulations & Results

First, we specify the simulation setup. For the PGLib OPF test cases, we then evaluate the distance to AC-feasibility and local optimality for the DC-OPF solution and solutions to the QC and SDP relaxations. We also study how these distances are correlated with the optimality gap. We use the DC-OPF as a computationally inexpensive benchmark. We next investigate the robustness and potential sub-optimality of penalization methods. Finally, we focus on warm-starting of non-convex solvers with solutions of inexact convex relaxations.

A. Simulation Setup

We use the implementations of the AC-OPF, DC-OPF, QC relaxation, and SDP relaxation provided in PowerModels.jl [24], a computationally efficient open-source implementation in Julia. In PowerModels.jl, we use KNITRO and IPOPT to solve the non-convex AC-OPF, MOSEK [25] to solve the DC-OPF and the SDP relaxation, and IPOPT to solve the QC relaxation. The analysis in this work uses the PGLib OPF Benchmarks v18.08 [18], in particular, the test cases ranging from 14 to 3120 buses under typical, congested, and small angle difference conditions. We exclude the test case *case2000_tamu* since the SDP relaxation fails for this test case. For the remaining 96 test cases, the QC and SDP relaxations return the optimal solution, although it should be noted that MOSEK reports "stall" in some of the test cases due to numerical issues. For the small angle difference conditions, the DC-OPF is infeasible for several instances. For these, we iteratively relax the angle difference constraints in the DC-OPF problem in 10% steps until we obtain a feasible solution. All simulations are carried out on a laptop with processor Intel(R) Core(TM) i7-7820HQ CPU @ 2.90 GHz and 32GB RAM.

B. Distances to AC-Feasibility and Local Optimality

1) AC-Feasibility: In the following, we evaluate the constraint violation resulting from AC power flow solutions in MATPOWER [26] obtained using the generators' setpoints for active power outputs and voltage magnitudes from the DC-OPF, QC relaxation, and SDP relaxation. For this purpose, we make the following assumptions: The largest generator is selected as slack bus. A numerical tolerance of 0.1% is considered as minimum constraint violation limit. Note that out of 96 test cases considered, the AC power flow does not converge for four test cases under any of the three loading conditions due to numerical ill-conditioning. The characteristics of these four test cases, which model parts of the French

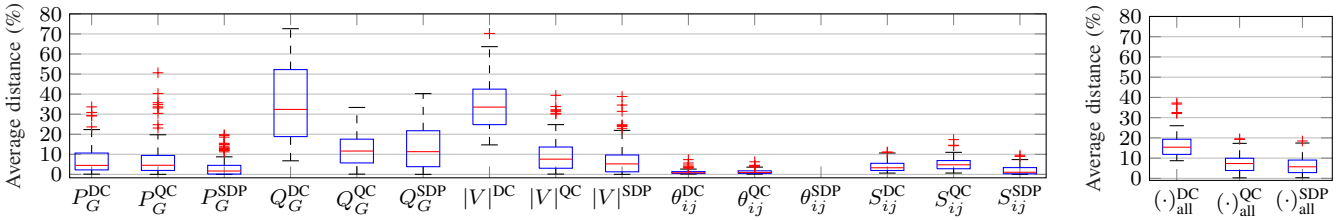

Fig. 2. Averaged normalized distance of the solution variables of the DC-OPF, QC and SDP relaxations to the locally optimal solution reported by IPOPT considering each state variable P_G, Q_G, $|V|$, Θ_{ij}, S_{ij} (left figure), and the evaluated distances averaged for all state variables (right figure).

transmission network, are detailed in [27]. These AC power flows also do not converge using PowerModels.jl with IPOPT. The underlying reasons for power flow non-convergence are outside the scope of this work. The following AC-feasibility analysis uses the results of the MATPOWER AC-PF and focuses on the remaining 84 convergent test cases.

In Fig. 1, we investigate the fraction of constraints violated and the cumulative constraint violation. In terms of fraction of constraints violated, the lower 75th percentiles for the QC and SDP relaxations (2.9% and 2.5%, respectively) are lower than for DC-OPF (4.2%). Regarding the cumulative constraint violation, the lower 25th percentile for the SDP relaxation (10.6%) is lower than the QC relaxation (33.1%) and the DC-OPF (232.6%), as these test cases are very close to a rank-1 solution. Furthermore, the lower 75th percentile of the cumulative constraint violation for the SDP and QC relaxations are 75.6% and 60.8% lower than for the DC-OPF, respectively, highlighting that the obtained solutions are closer to AC-feasibility. We also evaluate the type of constraint leading to the maximum constraint violation and we find that this is the generator reactive power in 71.1%, 50.6% and 49.4% of test cases for the DC-OPF, QC relaxation and SDP relaxation, respectively. If we enforce the reactive power limits in the AC-PF, whenever possible, active generator power and voltage limit violations occur more often instead. The cumulative constraint violation relates to the distance to an AC-feasible solution, which is not necessarily the same as the distance to a locally optimal solution. Therefore, we analyze the latter next.

2) Local Optimality: For the 96 considered test cases, we compute the average normalized distance between the locally optimal solution found by the non-convex solver IPOPT and the solutions to the DC-OPF, the QC relaxation, and the SDP relaxation. Fig. 2 shows the average distance for each state variable and for the average of all state variables. Considering all state variables, the lower 75th percentiles for the SDP and QC relaxations are less than 10% (9.0% and 9.9%), and significantly smaller than the DC-OPF solution (19.3%). Looking at the individual state variables, the SDP and QC relaxations' solutions are significantly closer to the local solution than the DC-OPF, particularly for the reactive generator power Q_G and voltage magnitude $|V|$. For generator active power and the apparent branch flow, the SDP relaxation is the closest (less than 5% for the lower 75th percentile). Since obtaining the voltage angles from the SDP relaxation's solutions is not straightforward, the angles are set to zero, and we do not report the distance in Fig. 2. The closeness of solutions from the QC and SDP relaxations relative to the local solution motivates our investigation of warm-starting techniques in Section V-D.

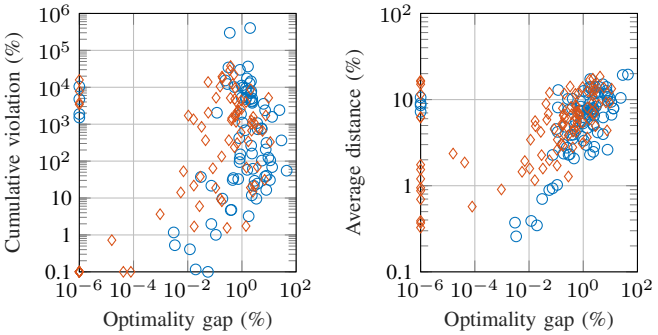

Fig. 3. Correlation of the optimality gap with the cumulative constraint violation and the averaged distance to local optimality for the QC and SDP relaxations. Note that the axes are logarithmic. The red diamonds correspond to the SDP relaxation, and the blue circles correspond to the QC relaxation.

3) Correlation with Optimality Gap: We investigate the correlation between the optimality gaps and both the averaged normalized distance and cumulative constraint violation for the QC and SDP relaxations as shown in Fig. 3. Note that both axes are on a logarithmic scale and the values are thresholded at 10^{-6}. We use the locally optimal solution obtained from IPOPT as the best known feasible point to compute the optimality gap. Even for cases with optimality gaps that are less than 1%, both the distances to local optimality and the cumulative constraint violations can still be substantial, suggesting that the optimality gap does not adequately capture the tightness of a relaxation in terms of the decision variable accuracy. Furthermore, there is a group of test cases with non-negligible distances to local optimality and substantial constraint violations that nevertheless have optimality gaps which are almost zero. The outliers are the following four test cases: *case2383wp_k__api*, *pglib_opf_case2746wop_k__api*, *case2746wp_k__api*, *case3012wp_k__api*, which are some of the test cases representing the Polish grid under congested operation conditions (api). A possible explanation is that the objective functions for these test cases is very flat with respect to the change in the active generator dispatch, e.g., there are many generators with similar costs.

For the correlation analysis, we use Spearman's rank and Pearson's correlation coefficient. The first coefficient relates to the (possibly non-linear) monotonicity of the optimality gap with the two metrics described in Section III. For the Pearson correlation coefficient, we identify the strength of possible linear relationships between the base-10 logarithms of the optimality gaps and these metrics. For both coefficients, the obtained values can range between -1 and 1, where the minimum and maximum values correspond to perfect negative or positive correlation, and the value of 0 expresses that the quantities are uncorrelated in this statistical measure. With

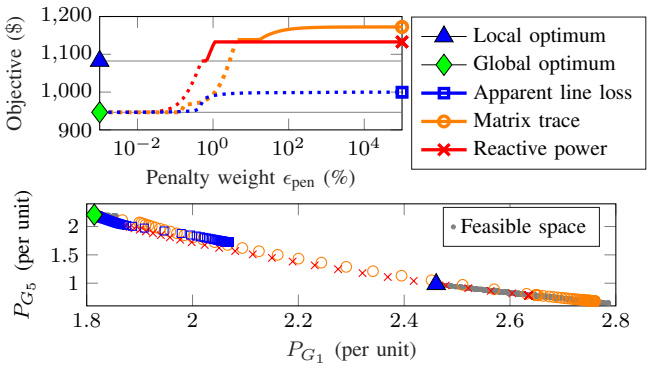

Fig. 4. The upper plot shows a comparison of penalization methods applied to the SDP relaxation for the five-bus test case from [28]. The solid lines represent the regions within which a rank-1 solution matrix is obtained and hence the SDP solution is AC-feasible. Conversely, the dotted lines correspond to higher-rank solution matrix for which the SDP solution is not AC-feasible. The two horizontal lines indicate the objective values of the local and global optima. The bottom plot shows the results from the penalization methods projected on the disconnected feasible space with respect to the active power generation P_{G_1} and P_{G_2}. The feasible space is reproduced from [29].

regard to both the cumulative constraint violation and the distance to local optimality metrics, the resulting Spearman's rank and Pearson correlation coefficients are in an interval between 0.03 and 0.57, showing that both metrics are not strongly correlated with the optimality gap.

C. Penalization Methods for SDP Relaxation

The previous section shows that the SDP relaxation's solution is close to both AC-feasibility and local optimality in various test cases. To drive the solution towards rank-1 and consequently AC-feasibility, we have presented three penalty terms from the literature in Section IV-A. In this section, we provide a detailed analysis of the robustness of these heuristic penalization methods for recovering an AC-feasible solution. We also quantify the sub-optimality incurred by modifying the original objective function. First, we present a five-bus test case serving as an illustrative example where penalty terms can fail to recover both an AC-feasible solution and a near-globally or locally optimal solution. Then, we provide a detailed numerical analysis on the PGLib OPF test case database considering all test cases with up to 300 buses. To facilitate comparability, as the absolute objective function values of the different test cases vary significantly, we define the penalty weight in percent of the original objective function value f^0_{cost} of the SDP relaxation with no penalty term included. As an illustrative example, a penalty weight of $\epsilon_{\text{pen}} = 1\%$ corresponds to $\epsilon_{\text{pen}} = 0.01 \times f^0_{\text{cost}}$. We use a heuristic measure for the rank-1 property of the obtained W matrix; specifically, that the ratio of first and second eigenvalues of the obtained W matrix should be larger than 1×10^4.

1) Five-Bus Test Case: We investigate the five-bus test case from [28]. The feasible space of this system is visualized in [29] and shown to be disconnected with one local solution in addition to the global optimum. The upper plot in Fig. 4 shows the objective value versus the penalty weight for the three different penalty functions. We use a penalty step size $\Delta\epsilon_{\text{pen}}$ of $10^{0.05}\%$ ranging from $10^{-3}\%$ to $10^{5}\%$. The solid line sections represent the region within which each penalty term yields a rank-1 solution matrix W. The lower plot in Fig. 4 shows the feasible space and the corresponding results of the penalization methods projected onto the disconnected feasible space with respect to the active power generation P_{G_1} and P_{G_2}. We make the following observations: The SDP relaxation without a penalty term included is inexact, but very close to the global optimum. Excluding the voltage angles (which are not available from the PowerModels.jl implementation), the normalized distances to the local and global optima are 4.2% and 0.1%, respectively. The MATPOWER AC-PF, however, does not converge if initialized with the solution of the inexact SDP relaxation. The performance of the three penalization terms is compared: By including a reactive power penalty, the solution is moving towards the local optimum and away from the global optimum. If the reactive power penalty weight is chosen high enough, we obtain a rank-1 matrix, represented by the solid part of the line, and we obtain the locally optimal solution for a small interval of penalty weights ($\epsilon_{\text{pen}} \approx 0.5\%$ to 0.7%). As we increase the penalty weight beyond 0.7%, the solution is driven towards a different rank-1 (and hence AC-feasible) point which incurs sub-optimalities of 19.7% and 4.7% for the globally and locally optimal solutions, respectively. For the matrix trace, a sufficiently high penalty term of 4.5% yields a rank-1 solution. In this case, we cannot obtain the locally optimal solution, but incur at least a sub-optimality of 20.3% and 5.2% with respect to the global and local optima, respectively. As seen in the plot of the feasible space, increasingly penalizing the matrix trace results in movement toward the same portion of the feasible space as increasing the reactive power penalty, but does not result in passing through the locally optimal solution. The apparent branch loss penalty term fails to recover a rank-1 solution for all considered penalty weights. As seen in the plot of the feasible space, increasing the apparent branch loss penalty results in movement towards the same portion of the feasible space, but remains AC-infeasible.

TABLE I
PERFORMANCE OF PENALIZATION METHODS ON PGLIB OPF TEST CASES

Penalty term	Add. rank-1 cases (%)	Range of $\epsilon^{\text{min}}_{\text{pen}}$ (%)	Min. opt. gap (%)	Range of $\epsilon^{\text{max}}_{\text{pen}}$ (%)	Max. opt. gap (%)
Q_G	42.2	10^{-5}–10^{9}	2.1	10^{10}	17.0
$\text{Tr}\{W\}$	22.2	10^{-5}–10^{7}	0.1	10^{4}–10^{10}	4.3
$\lvert S_{ij} - S_{ji}\rvert$	24.4	10^{-5}–10^{8}	2.5	10^{5}–10^{7}	4.2

2) PGLib OPF Test Cases up to 300 Buses: We investigate the performance of the three penalization methods on 45 PGLib-OPF test cases with up to 300 buses. Of these, the SDP relaxation is exact for 22.2%, i.e., an AC-feasible and globally optimal solution can be recovered. For the remaining 77.8% of test cases, we evaluate a wide range of penalty weights from $\epsilon_{\text{pen}} = \{10^{-5}, 10^{-4}, ..., 10^{9}, 10^{10}\}\%$ and determine the number of additional test cases for which a rank-1 solution can be recovered. For each successful test case, we evaluate the range of minimum and maximum penalty weights $\epsilon^{\text{min}}_{\text{pen}}$, $\epsilon^{\text{max}}_{\text{pen}}$ that allow recovery of a rank-1 solution and the minimum and maximum optimality gap with respect to the non-penalized objective value f^0_{cost} of the SDP relaxation. The results are shown in Table I. The penalty term for reactive power is the most effective at recovering rank-1 solutions. Specifically, rank-1 solutions are obtained for an additional 42.2% test

TABLE II
PGLIB OPF TEST INSTANCES SOLVED TO LOCAL OPTIMALITY (%)

Solver / Initialization	Flat start	DC-OPF	QC	SDP
KNITRO (SQP)	85.4	75.0	81.3	81.3
KNITRO (IPM)	99.0	92.7	97.9	93.8
IPOPT (IPM)	100.0	100.0	100.0	100.0

cases. Note that the test cases recovered by the apparent branch loss and the matrix trace are a subset of those recovered by the reactive power penalty. For the reactive power penalty in particular, the spread between the minimum and maximum optimality gap to obtain a rank-1 solution is 14.9%, ranging from 2.1% to 17.0%, indicating that a large sub-optimality can be incurred by assigning a sub-optimal penalty weight. Note the minimum penalty weight necessary to recover a rank-1 solution for the different test cases and different penalty terms varies considerably, with the interval for the minimum reactive power penalty $\epsilon_{\text{pen}}^{\text{min}}$ ranging from $10^{-5}\%$ to $10^{9}\%$. Since a detailed screening of a wide range of penalty terms is likely to be computationally prohibitive, these results highlight the challenge of choosing a penalty weight that both recovers a rank-1 solution and is small enough to obtain a near-globally optimal solution. Furthermore, in 35.6% of the test cases, none of these penalties successfully recover a rank-1 solution and the penalization heuristics fail to obtain an AC-feasible solution. Some works (e.g. [16]) propose using a combination of penalty terms with individual penalty weights to obtain an AC-feasible solution, which, however, leads to an exponential increase in possible penalty weight combinations.

D. Warm-Starting Non-Convex Solvers

This section investigates whether non-convex solvers can be efficiently warm-started in the search for local optima when initialized with solutions of convex relaxations. To this end, we use the SQP solver in KNITRO (algorithm 4), and the IPM solvers provided by KNITRO (algorithm 1) and IPOPT. We deactivated the presolve in KNITRO, as enabling the presolve resulted in significantly longer solver times. An upper time limit of 2000 seconds is enforced. For the remaining options, we use the default values. We first look at the solver reliability, then study the variation in computational speed for different initializations, and finally evaluate the solution quality.

1) Solver Reliability: Table II shows the share of the 96 considered PGLib OPF test instances which are solved to local optimality for the different initializations and solvers. IPOPT is the most reliable solver, with 100% of the test instances solved to local optimality irrespective of the initialization. The IPM and SQP solvers in KNITRO are less reliable, and achieve their highest reliability for the flat start initialization. For the other instances solved by KNITRO, either the time limit of 2000 seconds was reached or the solver reported local infeasibility.

2) Computational Speed: Fig. 5 shows the variation in computational speed relative to a flat start for the warm-started non-convex solvers initialized with the solutions to the DC-OPF and the QC and SDP relaxations. Note that we only consider instances solved to local optimality, and we do not include the computational time required to compute the initializations. Warm-starting can have a positive or negative

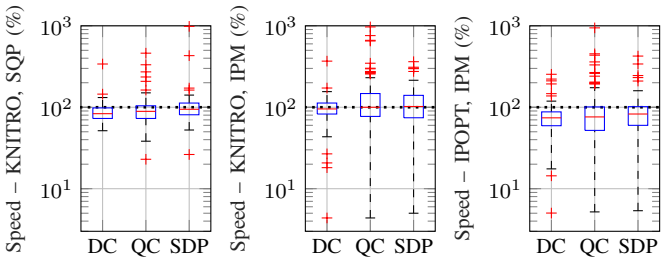

Fig. 5. Variation in computational speed relative to a flat start resulting from warm-starting the SQP solver in KNITRO, the IPM solver in KNITRO, and IPOPT using the solutions of the DC-OPF, the QC relaxation, and the SDP relaxation. Note the y-axis is shown on a logarithmic scale. The value of 100% (10^2%) corresponds to the computational speed of the flat start, with lower values indicating a speed improvement and higher values slower performance.

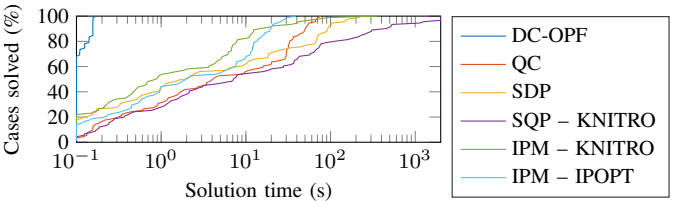

Fig. 6. PGLib OPF instances solved versus computational time for the DC-OPF, the QC and SDP relaxations as well as for the SQP solver in KNITRO, the IPM solver in KNITRO, and IPOPT when initialized with a flat start.

effect on computational speed for both solution methods and all three solvers. IPOPT shows the best performance with the lower 75th percentiles exhibiting speed improvements when initalized with solutions to the DC-OPF and the QC and SDP relaxations as well as median speed improvements of 25.8% for DC-OPF, 23.9% for the QC relaxation, and 17.4% for the SDP relaxation. This does not confirm that SQP methods are usually more suitable for warm-starting as stated in Section IV-B. The IPM solver in KNITRO performs worse, with only the lower 50th percentile of test cases exhibiting a speed improvement. The SQP solver in KNITRO has better computational speed than the IPM solver in KNITRO but has significantly lower solver reliability as shown in Table II. Both the Pearson's and Spearman's rank correlation coefficients for the computational speed-up and the i) optimality gaps, ii) cumulative constraint violations, and iii) the distances to local optimality lie in a range between -0.22 and 0.49, thus showing that these three metrics are not strongly correlated with the computational speed-up in these statistical measures.

Fig. 6 shows the solution times of all the non-convex solvers initalized with a flat start and of the DC-OPF, the QC relaxation, and the SDP relaxation. The DC-OPF is by far the fastest, as it involves only solving an LP or QP. The SDP relaxation in PowerModels.jl is faster than the QC relaxation for small and medium systems but is approximately an order-of-magnitude slower for large systems. It can be observed that interior-point solvers, in particular IPOPT, are significantly faster than SQP solvers for the AC-OPF problem as the SQP solvers do not scale well with increasing system size.

3) Solution Quality: For the evaluated cases, all non-convex solvers which converge to local optimality from all starting points obtain the same objective value to within a small numerical tolerance of 10^{-5}. For the five-bus test case from [28] discussed earlier, IPOPT and the SQP solver in KNITRO

return the locally optimal solution when initialized with the flat start. All warm-started local solvers return the globally optimal solution to this problem; thus, in this case, warm-starting the solvers yields an improvement in solution quality.

VI. Conclusions and Outlook

Using the PGLib OPF benchmarks from [18], we provided a comprehensive study regarding the distance of the inexact solutions to the QC relaxation and the SDP relaxation relative to both AC-feasibility and local optimality for the original non-convex AC-OPF problem. In addition, we investigated two methods for recovering AC-feasible or locally optimal solutions: penalization methods and warm-starting of non-convex solvers. Based on our detailed results, we summarize our main conclusions and outline directions for further research:

1) To quantify the distance to AC-feasibility and local optimality, we proposed two empirical metrics to complement the optimality gap for analyzing the relaxations' accuracy. For both the QC and SDP relaxations, we have shown that the distances to both AC-feasibility and local optimality are small for the majority of test cases. Furthermore, these metrics are not strongly correlated with the optimality gap, and despite an optimality gap of less than 1%, several test cases still exhibit a substantial distance to AC-feasibility and local optimality. Detailed investigations of these cases and of four outliers could provide additional insights into the QC and SDP relaxations.

2) Heuristic penalization methods for the SDP relaxation can be successful in recovering an AC-feasible and near-globally optimal solution. However, choosing an appropriate penalty weight can be challenging since detailed screenings of a wide range of penalty terms might be computationally prohibitive. Furthermore, there exists a range of test cases for which all investigated penalization methods fail to recover an AC-feasible solution. Therefore, systematic methods to choose the penalty weight and penalty term are necessary, and successive penalization methods such as those recently proposed in [30] could provide a further research direction.

3) We investigated warm-starting non-convex solvers with the solutions of the inexact convex relaxations. We have shown that the sequential quadratic programming solver in KNITRO is not scalable to large instances and exhibits issues with solver convergence when warm started. Conversely, the interior-point solver in IPOPT is highly reliable and computationally efficient: in more than 75% of the considered PGLib OPF test cases, a computational speed-up can be achieved by warm-starting with the solution of an inexact convex relaxation. A future direction is to improve the warm-starting of the interior-point method by a) decreasing the initial logarithmic barrier term in the objective function and b) using dual information.

References

[1] P. Panciatici *et al.*, "Advanced Optimization Methods for Power Systems," in *18th Power Systems Computation Conference (PSCC)*, 2014.

[2] K. Lehmann, A. Grastien, and P. V. Hentenryck, "AC-Feasibility on Tree Networks is NP-Hard," *IEEE Transactions on Power Systems*, vol. 31, no. 1, pp. 798–801, 2016.

[3] K. Dvijotham and D. Molzahn, "Error Bounds on the DC Power Flow Approximations: A Convex Relaxation Approach," *IEEE 55th Conference on Decision and Control (CDC)*, December 2016.

[4] R. Jabr, "Radial Distribution Load Flow using Conic Programming," *IEEE Transactions on Power Systems*, vol. 21, no. 3, pp. 1458–1459, 2006.

[5] X. Bai, H. Wei, K. Fujisawa, and Y. Wang, "Semidefinite Programming for Optimal Power Flow Problems," *International Journal of Electrical Power & Energy Systems*, vol. 30, no. 6-7, pp. 383–392, 2008.

[6] J. Lavaei and S. H. Low, "Zero Duality Gap in Optimal Power Flow Problem," *IEEE Transactions on Power Systems*, vol. 27, no. 1, pp. 92–107, Feb 2012.

[7] C. Coffrin, H. L. Hijazi, and P. Van Hentenryck, "The QC Relaxation: A Theoretical and Computational Study on Optimal Power Flow," *IEEE Transactions on Power Systems*, vol. 31, no. 4, pp. 3008–3018, 2016.

[8] D. K. Molzahn and I. A. Hiskens, "A Survey of Relaxations and Approximations of the Power Flow Equations," *Foundations and Trends in Electric Energy Systems*, vol. 4, no. 1-2, pp. 1–221, 2019.

[9] D. K. Molzahn, J. T. Holzer, B. C. Lesieutre, and C. L. DeMarco, "Implementation of a Large-Scale Optimal Power Flow Solver based on Semidefinite Programming," *IEEE Transactions on Power Systems*, vol. 28, no. 4, pp. 3987–3998, 2013.

[10] A. Eltved, J. Dahl, and M. S. Andersen, "On the Robustness and Scalability of Semidefinite Relaxation for Optimal Power Flow Problems," *arXiv:1806.08620*, 2018.

[11] D. K. Molzahn *et al.*, "A Survey of Distributed Optimization and Control Algorithms for Electric Power Systems," *IEEE Transactions on Smart Grid*, vol. 8, no. 6, pp. 2939–2940, Nov. 2017.

[12] D. K. Molzahn and L. A. Roald, "Towards an AC Optimal Power Flow Algorithm with Robust Feasibility Guarantees," in *20th Power Systems Computation Conference (PSCC)*, June 2018.

[13] A. Lorca and X. A. Sun, "The Adaptive Robust Multi-Period Alternating Current Optimal Power Flow Problem," *IEEE Transactions on Power Systems*, vol. 33, no. 2, pp. 1993–2003, March 2018.

[14] D. K. Molzahn and I. A. Hiskens, "Sparsity-Exploiting Moment-Based Relaxations of the Optimal Power Flow Problem," *IEEE Transactions on Power Systems*, vol. 30, no. 6, pp. 3168–3180, 2015.

[15] R. Madani, S. Sojoudi, and J. Lavaei, "Convex Relaxation for Optimal Power Flow Problem: Mesh Networks," *IEEE Transactions on Power Systems*, vol. 30, no. 1, pp. 199–211, January 2015.

[16] R. Madani, M. Ashraphijuo, and J. Lavaei, "Promises of Conic Relaxation for Contingency-Constrained Optimal Power Flow Problem," *IEEE Transactions on Power Systems*, vol. 31, no. 2, pp. 1297–1307, 2016.

[17] A. Venzke *et al.*, "Convex Relaxations of Chance Constrained AC Optimal Power Flow," *IEEE Transactions on Power Systems*, vol. 33, no. 3, pp. 2829–2841, 2018.

[18] The IEEE PES Task Force on Benchmarks for Validation of Emerging Power System Algorithms, "PGLib Optimal Power Flow Benchmarks," Published online at https://github.com/power-grid-lib/pglib-opf, 2018.

[19] A. Wächter and L. T. Biegler, "On the Implementation of an Interior-Point Filter Line-Search Algorithm for Large-Scale Nonlinear Programming," *Mathematical programming*, vol. 106, no. 1, pp. 25–57, 2006.

[20] M. Fazel, H. Hindi, and S. P. Boyd, "A Rank Minimization Heuristic with Application to Minimum Order System Approximation," in *American Control Conference (ACC)*, vol. 6. IEEE, 2001, pp. 4734–4739.

[21] P. E. Gill and E. Wong, "Sequential Quadratic Programming Methods," in *Mixed Integer Nonlinear Programming*. Springer, 2012, pp. 147–224.

[22] R. H. Byrd, J. Nocedal, and R. A. Waltz, "Knitro: An Integrated Package for Nonlinear Optimization," in *Large-Scale Nonlinear Optimization*. Springer, 2006, pp. 35–59.

[23] A. Forsgren, "On Warm Starts for Interior Methods," in *IFIP Conference on System Modeling and Optimization*. Springer, 2005, pp. 51–66.

[24] C. Coffrin, R. Bent, K. Sundar, Y. Ng, and M. Lubin, "PowerModels.jl: An Open-Source Framework for Exploring Power Flow Formulations," in *20th Power Systems Computation Conference (PSCC)*, June 2018.

[25] MOSEK ApS, *MOSEK 8.0.0.37* , 2018.

[26] R. D. Zimmerman, C. E. Murillo-Sánchez, and R. J. Thomas, "MATPOWER: Steady-State Operations, Planning, and Analysis Tools for Power Systems Research and Education," *IEEE Transactions on Power Systems*, vol. 26, no. 1, pp. 12–19, 2011.

[27] C. Josz, S. Fliscounakis, J. Maeght, and P. Panciatici, "AC power flow data in MATPOWER and QCQP format: iTesla, RTE snapshots, and PEGASE," *arXiv:1603.01533*, 2016.

[28] W. A. Bukhsh, A. Grothey, K. I. M. McKinnon, and P. A. Trodden, "Local Solutions of the Optimal Power Flow Problem," *IEEE Transactions on Power Systems*, vol. 28, no. 4, pp. 4780–4788, Nov 2013.

[29] D. K. Molzahn, "Computing the Feasible Spaces of Optimal Power Flow Problems," *IEEE Transactionson Power Systems*, vol. 32, no. 6, pp. 4752–4763, November 2017.

[30] W. Wei, J. Wang, N. Li, and S. Mei, "Optimal Power Flow of Radial Networks and Its Variations: A Sequential Convex Optimization Approach," *IEEE Transactions on Smart Grid*, vol. 8, no. 6, pp. 2974–2987, 2017.